Acta geographica Slovenica, 64-3, 2024, 75–95

MONITORING THE IMPACT OF THE CORONA PANDEMIC ON NITROGEN DIOXIDE EMISSIONS AT LARGE SCALES VIA GOOGLE EARTH ENGINE

Nuri Erkin Öçer, Dilek Küçük Matcı, Uğur Avdan

ESA/NASA

The monitoring of vast expanses is a key function of Earth observation satellites.

DOI: https://doi.org/10.3986/AGS.13454
UDC: 528.8:913”2019/2021”

Nuri Erkin Öçer[1], Dilek Küçük Matcı[1], Uğur Avdan[1]

Monitoring the impact of the Corona pandemic on nitrogen dioxide emissions at large scales via Google Earth Engine

ABSTRACT: Advances in Earth observation capabilities and the expanded accessibility of data provide the opportunity to monitor air pollution on a global scale. The Google Earth Engine (GEE) enables the efficient conduct of such large-scale research. This article examines the impact of the COVID-19 pandemic on NO_2 emissions at various supranational scales, with particular consideration of the Human Development Index of the countries, using GEE. The findings for the first three months of 2020 indicating a reduction in emissions of more than 4% per month, demonstrate that not only were the restrictions and closures imposed by governments effective in the global decline of NO_2 levels, but also voluntary restrictions imposed by people on their own mobility with the motive of protection from the pandemic.

KEYWORDS: remote sensing, Earth observation, Sentinel-5P, tropospheric NO_2, Google Earth Engine, Human Development Index

Spremljanje vpliva pandemije koronavirusa na emisije dušikovega dioksida v velikem merilu s programom Google Earth Engine

POVZETEK : Napredek v zmogljivostih opazovanja Zemlje in večja dostopnost podatkov omogočata spremljanje onesnaženosti zraka na svetovni ravni. Google Earth Engine (GEE) omogoča učinkovito izvajanje takšnih obsežnih raziskav. Ta članek z uporabo GEE preučuje vpliv pandemije covida-19 na emisije NO_2 na različnih nadnacionalnih ravneh, s posebnim upoštevanjem indeksa človekovega razvoja v državah. V prvih treh mesecih leta 2020 je prišlo do zmanjšanja za več kot 4 % na mesec, kar kaže, da pri globalnem zmanjšanju ravni NO_2 niso bile učinkovite le omejitve in zaprtja, ki so jih uvedle vlade, temveč tudi prostovoljne omejitve, ki so jih ljudje uvedli za lastno mobilnost z motivom zaščite pred pandemijo.

KLJUČNE BESEDE: daljinsko zaznavanje, opazovanje Zemlje, Sentinel-5P, troposferski NO_2, Google Earth Engine, indeks človekovega razvoja

The article was submitted for publication on December 14th, 2023.
Uredništvo je prejelo prispevek 14. decembra 2023.

[1] Eskisehir Technical University, Earth and Space Sciences Institute, Eskisehir, Turkey
neocer@eskisehir.edu.tr (https://orcid.org/0000-0001-7404-7686), dkmatci@eskisehir.edu.tr (https://orcid.org/0000-0002-4078-8782), uavdan@eskisehir.edu.tr (https://orcid.org/0000-0001-7873-9874)

1 Introduction

First reported in Wuhan, China, in January 2020, the COVID-19 epidemic spread rapidly around the world. Soon after the outbreak, almost every country introduced various measures to contain the spread of the disease, including travel restrictions and curfews, with varying degrees of severity (Hale et al. 2021; Singh and Chauhan 2020). Some governments implemented a complete quarantine, while others opted for partial lockdowns or mobility restrictions (Zhang et al. 2021). For instance, while the Chinese central government implemented a complete shutdown in Wuhan, the Turkish government enacted a nationwide but partial shutdown (Bacak et al. 2020; Lian et al. 2020). The implementation of these measures has resulted in a notable decline in human mobility. Since the majority of air pollutants are of anthropogenic origin and closely related to human mobility, there has also been a significant reduction in air pollution during the pandemic period. For example, Tobías et al. (2020) observed a notable decline in PM10, NO_2, SO_2 and CO levels in Barcelona during the one-month quarantine period. Isaifan (2020) also demonstrated a significant reduction in NO_2 and carbon emissions associated with quarantines in China. Karuppasamy et al. (2020) observed a 55% reduction in NO_2 during the period of quarantine in India. Another study (Otmani et al. 2020) revealed reductions of 75%, 49% and 96% in PM10, SO_2 and NO_2, respectively, in Morocco. Moreover, a significant reduction in air pollution was reported in Iran during the outbreak (Nemati et al. 2020).

The majority of the studies mentioned above employed air quality monitoring stations (terrestrial instruments) to assess air quality. Such instruments are capable of taking point measurements with high temporal resolution, rendering them suitable for use in situations where ambient change is rapid. Nevertheless, they lack convenience and practicality, as they necessitate the deployment of a substantial number of instruments to collect data on extensive areas. For instance, Karuppasamy et al. (2020) employed data from over 12,000 stations in a global-scale study. In contrast, airborne or spaceborne remote sensing instruments are capable of providing information on large areas of the Earth's surface, albeit at less frequent intervals. These tools provide valuable, easily accessible and reliable data for studies in a multitude of fields (Avdan et al. 2021; Kuruca et al. 2021; Matcı and Avdan 2020; Matci et al. 2020; Praticò et al. 2021; Tok and Kaya 2014; Zhe 2018). One such tool is the TROPOspheric Monitoring Instrument (TROPOMI), developed by the European Space Agency with the objective of monitoring and predicting air quality, ozone, radiation and climate. It is an instrument on the Copernicus Sentinel-5 Precursor satellite that provides high spatial and temporal resolution data on tropospheric concentrations of ozone (O_3), methane (CH_4), formaldehyde (HCHO), carbon monoxide (CO), nitrogen dioxide (NO_2) and sulphur dioxide (SO_2) in netCDF (Network Common Data Form) format since July 10th, 2018. All Sentinel-5P data is freely available from The Copernicus Data Space Ecosytem in near real-time and offline.

One Sentinel-5P image encompasses approximately 100 million square kilometres of the Earth's surface and occupies over 500 megabytes of memory space. This implies that a one-year survey of the entire Earth utilising Sentinel-5P products as data would necessitate approximately 65,000 images and in excess of 30 terabytes of storage. Conducting such a survey in the traditional manner, by accessing, downloading and processing data one at a time, is a highly time-consuming, resource-intensive, and error-prone process. However, these issues can be overcome using Google Earth Engine (GEE), a cloud-based computing platform designed primarily for the analysis of Earth-scale environmental data. It combines petabytes of satellite imagery and geospatial datasets and allows users to easily access, process and visualize them (Kumar and Mutanga 2019). GEE has been applied and its capabilities explored in various fields related to earth sciences (Jalayer et al. 2023; Nejad et al. 2022; Nghia et al. 2022; Waleed et al. 2023; Xiong et al. 2017). The impact of the coronavirus pandemic on air pollution parameters such as tropospheric NO_2 levels has also been investigated in this way using Sentinel-5P data by Sannigrahi et al. (2021) and Sharifi and Felegari (2022). These city-scale studies, which also utilised in-situ data from ground stations, demonstrated improvements in air quality in various cities during the pandemic.

Although the effects of pandemic lockdowns on NO_2 concentrations and distributions have been demonstrated at various scales, there is no study examining the changes in countries with different levels of development. In order to conduct such a study, it is necessary to determine the category boundaries according to a development index, rather than an administrative criterion. One such index is the Human Development Index (HDI), a measure of the level of development of countries, which has been calculated by the United Nations Development Programme (UNDP) for almost every country since 1990. A number of parameters, including life expectancy, health, access to education and per capita income, are taken into account in the calculation

of the HDI. The HDI has been employed in a multitude of academic contexts, including investigations into its correlation with health, obesity, CO_2 emissions, and the economy (Ataey et al. 2020; Long et al. 2020; Sarkodie and Adams 2020).

The primary objective of this study is to ascertain the extent to which tropospheric NO_2 concentrations are influenced by pandemic measures implemented by countries with disparate Human Development Index (HDI) categories. In order to achieve this objective, tropospheric NO_2 concentrations for the entire Earth were obtained using Sentinel-5P data through GEE for the years 2019, 2020 and 2021. The NO_2 levels are then evaluated and interpreted for countries grouped by HDI. Furthermore, the study encompasses the temporal variation of NO_2 concentrations over the specified period across the globe, geographical continents, and three neighbouring Southern European countries with disparate HDI categories (Slovenia, Croatia and Bosnia and Herzegovina).

2 Materials and methods

In this study, tropospheric NO_2 concentrations over the study areas between 2019 and 2021 were determined by utilising Sentinel-5P's TROPOMI NRTI NO_2: Near Real-Time Nitrogen Dioxide data, provided by the Copernicus Data Space Ecosystem through GEE. The product calculates tropospheric NO_2 concentrations by subtracting stratospheric contributions from the total columns. The TROPOMI/Sentinel-5P instrument, with a swath width of 108° (approximately 2,600 km on the ground), provides daily coverage of over 95% of the Earth's surface. The spatial resolution of the product is 5.5 km in the satellite flight direction and 3.5 km in the perpendicular direction at nadir. However, data released prior to August 6th, 2019 had a resolution up to 7.0 km in the flight direction. Statistical analyses of the comparison between TROPOMI and ground-based measurements (e.g., ZSL-DOAS SAOZ NO_2 data) demonstrate an excellent correlation (correlation coefficient = 0.94) between the two data sets. Furthermore, the histogram of the differences exhibits an almost Gaussian shape, with a small negative bias for TROPOMI (Verhoelst et al. 2020). The methodology in this study, developed entirely on the GEE platform, is schematised in Figure 1 and has been applied on various large-scale study areas. The methodology comprises three principal stages: data acquisition, pre-processing and processing. The process commences with the introduction of the study area to the software. In the study, the boundaries of the study areas are in geospatial vector data (shapefile) format. The boundaries of the HDI classes were delineated using the borders of each country and the respective HDI values. Subsequently, Sentinel-5P Level 3 data is accessed from the GEE data archive and the NRTI NO_2 band is selected. Due to the fact that pixels in Level 2 data are defined by latitude and longitude, it is difficult to combine multiple images in this type of data. Conversely, Level 3 data products are obtained by resampling the Level 2 ones to regular spatial pixel grids, rendering them suitable for combining. In the following stage, a time series of NRTI NO_2 is constructed by collecting the data acquired within the specified temporal range. The study employs monthly and annual time intervals. The process concludes with the calculation of the average of the time series, producing a map of the time-averaged NO_2 values of the study area.

The present study examines tropospheric NO_2 levels in the following study areas: the Earth, the continents, countries grouped according to HDI, and the triad of Slovenia, Croatia, and Bosnia and Herzegovina. Figure 2 provides a visual representation of the study areas. The investigation encompasses almost the entire Earth (including seas and oceans) with the exception of Antarctica. In the HDI-related part of the study, countries were examined by dividing them into categories of *Very High*, *High*, *Medium* and *Low* developed in accordance with the UNDP Reports catalogue for the year 2019 (the *Others* category was omitted). The list of countries, as classified by HDI, is presented in Table 1.

The study was conducted on a computer equipped with an Intel i9 7900X CPU (Central Processing Unit), an Nvidia GTX 1080 GPU (Graphics Processing Unit), 128 GB of Random-Access Memory (RAM), and a 1000 Mbps internet connection speed. In order to calculate the one-year average NO_2 for the largest study area, that of the Earth, a total of 64,188 Sentinel-5P images were used. The processing time was approximately 60 seconds.

The limitations of the methodology employed in this study can be considered from two distinct perspectives: data resolution and computational complexity. As the method is reliant on TROPOMI data for the measurement of atmospheric NO_2 emissions, the spatial resolution of the data is $3.5 \times 7.0\,km^2$ until

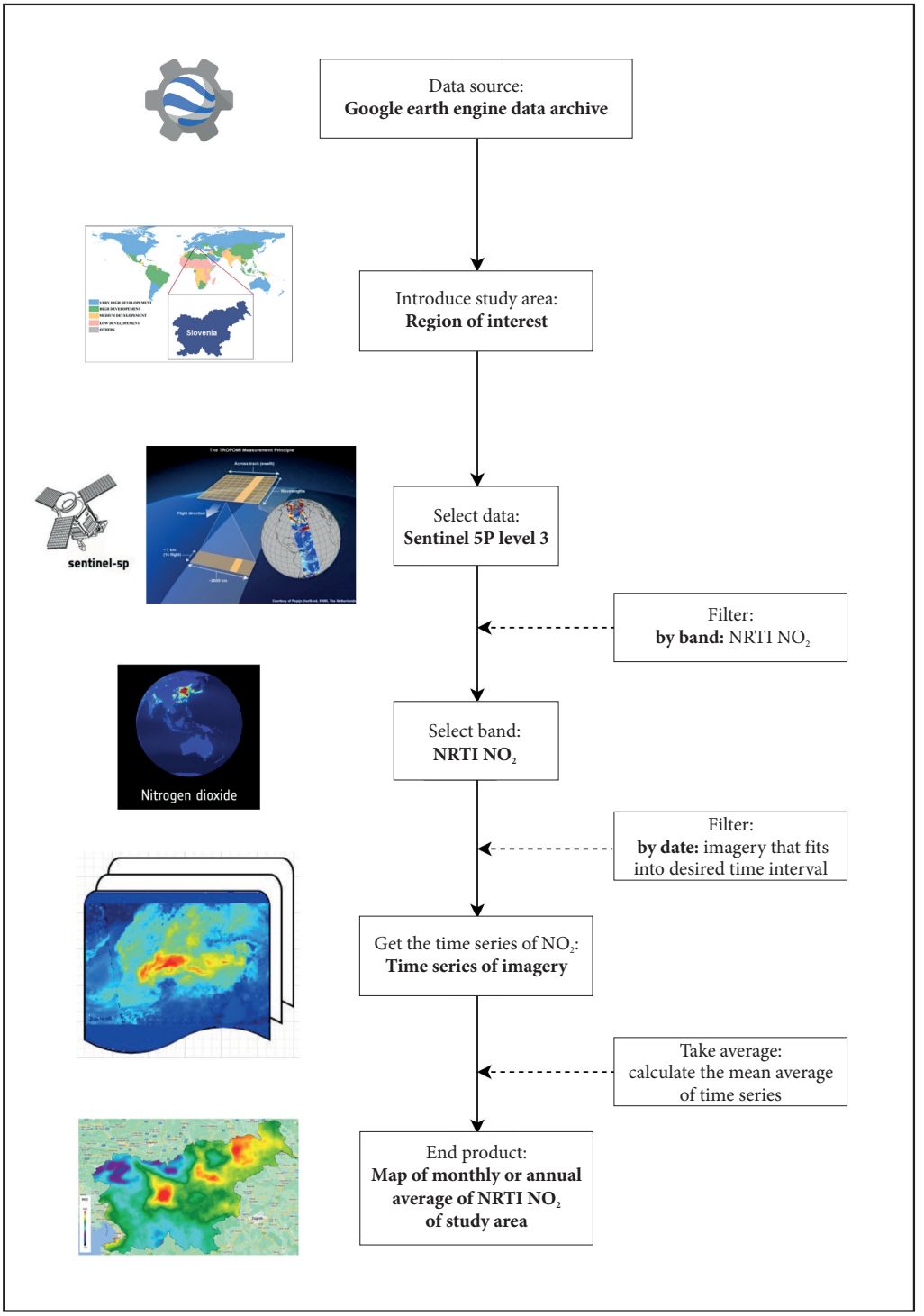

Figure 1: The workflow of the presented method.

August 6th, 2019 and $3.5 \times 5.0\ km^2$ thereafter. Therefore, it is not possible to capture changes at finer scales. Nevertheless, these data, which are highly correlated with reliable ground measurements in previous studies, are still useful for examining relative variability and trend analysis between years and months.

Furthermore, the algorithm employed in this study is only capable of handling shapefiles of the study areas up to a specific fineness of resolution, contingent on the size of RAM available. In this study, the algorithm, which was executed on a computer with 128 GB of RAM, was capable of processing shapefiles with a maximum resolution of 500 metres. For finer, more detailed shapefiles, the available memory was insufficient.

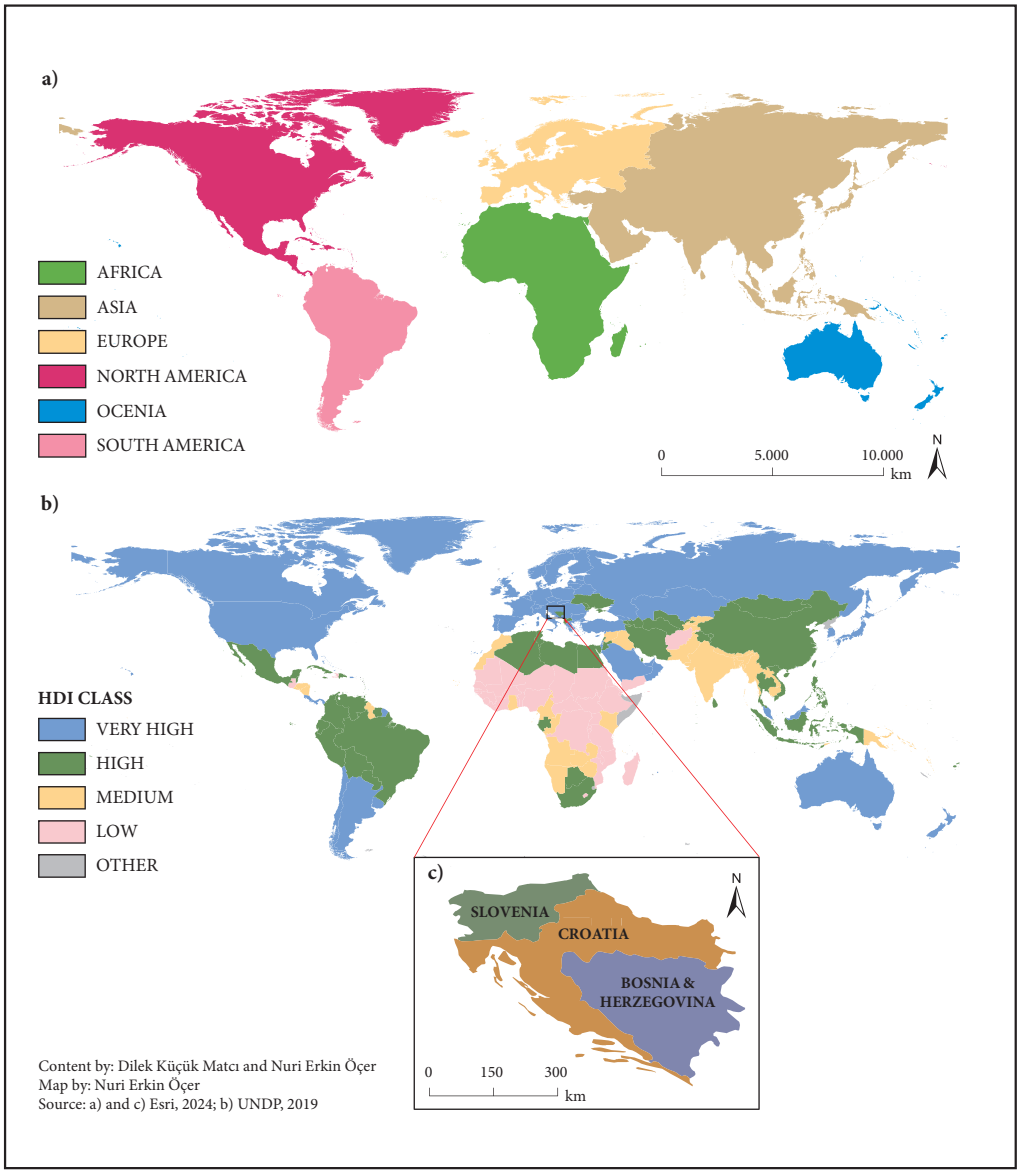

Figure 2: The study areas: a) the geographic continents, b) countries grouped according to HDI, c) the triad of Slovenia, Croatia, Bosnia and Herzegovina.

Table 1: The countries as grouped according to HDI for the year 2019.

Very High	Andorra	Very High	Portugal	High	Palestine, State of	Medium	Papua New Guinea
	Argentina		Qatar		Paraguay		Sao Tome and Principe
	Australia		Romania		Peru		Solomon Islands
	Austria		Russian Federation		Philippines		Syrian Arab Republic
	Bahamas		Saudi Arabia		Saint Kitts and Nevis		Tajikistan
	Bahrain		Serbia		Saint Lucia		Timor-Leste
	Barbados		Singapore		Saint Vincent and the Grenadines		Vanuatu
	Belarus		Slovakia		Samoa		Zambia
	Belgium		Slovenia		Seychelles		Zimbabwe
	Brunei Darussalam		Spain		South Africa	Low	Afghanistan
	Bulgaria		Sweden		Sri Lanka		Benin
	Canada		Switzerland		Suriname		Burkina Faso
	Chile		Turkey		Thailand		Burundi
	Costa Rica		United Arab Emirates		Tonga		Central African Republic
	Croatia		United Kingdom		Trinidad and Tobago		Chad
	Cyprus		United States		Tunisia		Congo (Dem.Rep. of the)
	Czechia		Uruguay		Turkmenistan		Côte d'Ivoire
	Denmark	High	Albania		Ukraine		Djibouti
	Estonia		Algeria		Uzbekistan		Eritrea
	Finland		Antigua and Barbuda		Venezuela (Bolivarian Rep. of)		Ethiopia
	France		Armenia		Viet Nam		Gambia
	Georgia		Azerbaijan	Medium	Angola		Guinea
	Germany		Belize		Bangladesh		Guinea-Bissau
	Greece		Bolivia		Bhutan		Haiti
	Hong Kong, China (SAR)		Bosnia and Herzegovina		Cabo Verde		Lesotho
	Hungary		Botswana		Cambodia		Liberia
	Iceland		Brazil		Cameroon		Madagascar
	Ireland		China		Comoros		Malawi
	Israel		Colombia		Congo		Mali
	Italy		Cuba		El Salvador		Mauritania
	Japan		Dominica		Equatorial Guinea		Mozambique
	Kazakhstan		Dominican Republic		Eswatini (Kingdom of)		Niger
	Korea (Republic of)		Ecuador		Ghana		Nigeria
	Kuwait		Egypt		Guatemala		Rwanda
	Latvia		Fiji		Guyana		Senegal
	Liechtenstein		Gabon		Honduras		Sierra Leone
	Lithuania		Grenada		India		South Sudan
	Luxembourg		Indonesia		Iraq		Sudan
	Malaysia		Iran (Islamic Republic of)		Kenya		Tanzania (United Republic of)
	Malta		Jamaica		Kiribati		Togo
	Mauritius		Jordan		Kyrgyzstan		Uganda
	Montenegro		Lebanon		Lao People's Democratic Rep.		Yemen
	Netherlands		Libya		Micronesia (Federated States of)	Others	Korea (Dem. People's Rep. of)
	New Zealand		Maldives		Morocco		Monaco
	Norway		Marshall Islands		Myanmar		Nauru
	Oman		Mexico		Namibia		San Marino
	Palau		Moldova (Republic of)		Nepal		Somalia
	Panama		Mongolia		Nicaragua		Tuvalu
	Poland		North Macedonia		Pakistan		

3 Results and discussion

The results obtained by the method employed are presented in this section in the form of maps and tables. The maps illustrate the distributions of the annual averages of tropospheric NO_2 column concentrations, while the tables show the annual and the monthly average values over each study area. The results are presented in the following order: the Earth, the geographical continents, the countries grouped according to HDI, and the triad of Slovenia, Croatia, Bosnia and Herzegovina.

3.1 NO_2 emission across the Earth

The distribution of the annual averages of the Earth's tropospheric NO_2 column concentrations for the years 2019, 2020 and 2021, are presented in Figure 3. The maps, each of which is an average of more than 64,000 images (occupying more than 30 terabytes of memory) recorded by the satellite throughout the study period, reveal the concentrations and distributions of tropospheric NO_2 worldwide before, during and after the pandemic, respectively. A visual comparison of the data reveals a significant decrease in the average NO_2 emission in the pandemic year (2020). This result is corroborated by Table 2, which presents the annual averages of tropospheric NO_2 concentrations for the study period across all study areas. For the Earth, the total NO_2 concentration decreased by 3.4% in 2020 (51.2 μmol/m²) in comparison to 2019 (53.0 μmol/m²), and then increased by 2.9% in 2021 (52.7 μmol/m²) in comparison to 2020. This represents a net decrease of 0.6% in the average concentration of NO_2 in 2021 in comparison to 2019.

The outcomes are in line with the results of the study of Saha et al. (2022), which compiled worldwide research on air quality parameters. They reported a significant improvement in global air pollution levels during the quarantine period and indicated the extent to which concentrations of major air pollutants, such as NO_2, SO_2, CO and particulate matter, decreased in major countries of the world. Furthermore, Cooper et al. (2022) employed a method that enabled them to quantify changes in NO_2 concentrations across more than 200 cities. Their results demonstrated that countries with stringent lockdown policies exhibited NO_2 concentration levels that were on average approximately 30% lower than in those without. Furthermore, the study revealed that the sensitivity of atmospheric NO_2 to closures exhibited variability across countries and emission sectors.

Table 2: The annual averages of NO_2 column concentrations for the Earth, the continents, the countries grouped according to HDI and the triad of Slovenia, Croatia, Bosnia and Herzegovina for the years of 2019, 2020 and 2021, and the change between years.

		NO_2 Column Density (μmol/m²)			Yearly Change (%)		
	Study Area	2019	2020	2021	2020–2019	2021–2020	2021–2019
	The Earth	53.0	51.2	52.7	–3.4	2.9	–0.6
The Continents	Africa	51.8	51.3	54.0	–1.0	5.3	4.2
	Asia	65.5	61.5	65.8	–6.1	7.0	0.5
	Europe	73.9	67.5	73.7	–8.7	9.2	–0.3
	North America	56.8	54.1	55.8	–4.8	3.1	–1.8
	Oceania	52.7	53.2	51.8	0.9	–2.6	–1.7
	South America	45.2	46.8	47.4	3.5	1.2	4.8
HDI Classes	Very High HDI	61.4	58.3	61.0	–5.1	4.7	–0.6
	High HDI	60.2	58.0	61.3	–3.7	5.7	1.9
	Medium HDI	57.4	56.3	59.8	–2.0	6.2	4.1
	Low HDI	49.6	48.9	52.4	–1.5	7.2	5.6
	Slovenia	80.7	76.0	83.9	–5.9	10.5	4.0
	Croatia	74.4	69.9	76.6	–6.1	9.6	3.0
	Bosnia and Her.	68.9	64.6	71.2	–6.3	10.3	3.4

Figure 3: The global distribution of annual averages of NO_2 column concentration for the years 2019 (top), 2020 (middle), and 2021 (bottom). ► p. 83

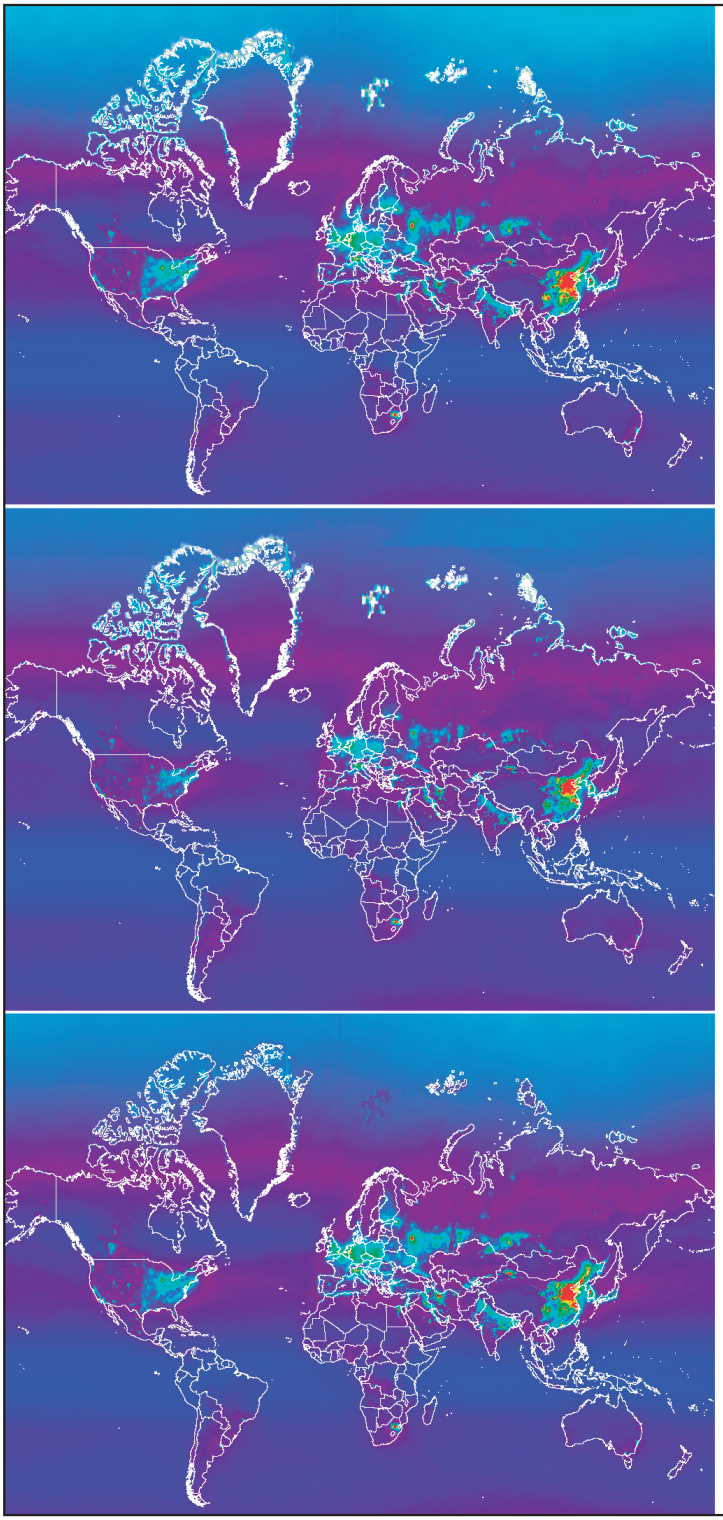
NO_2 Column Concentration (µmol/m²)
50
90
180
Scale: 1: 90,000.000
Content By: Dilek Küçük Matcı
and Nuri Erkin Öçer
Map By: Nuri Erkin Öçer
Source: Copernicus Data
Space Ecosystem, 2024

The variation in the monthly averages of NO_2 emissions for the Earth is presented in Table 3 and Figure 4. Accordingly, the mean NO_2 emissions for each month of 2020 were consistently lower than those for each month of 2019. Moreover, the results demonstrate that NO_2 levels were lower than the pre-pandemic values even before the countries adopted the pandemic closures and restriction measures, namely before mid-March. During the course of 2020, which encompassed a series of closures and the implementation of stringent measures, the tropospheric NO_2 concentration exhibited a decrease of 3.4% per month in comparison to the preceding year. In contrast, prior to the implementation of government measures, namely in the first three months of 2020, there was a monthly decrease of 4.0% in comparison to the corresponding period of the previous year. This can be interpreted as a result of individuals voluntarily limiting their movements and spending more time at home in order to protect themselves from the effects of pandemic. In 2021, following the relaxation of restrictions, monthly averages increased in all months except January in comparison to 2020.

Table 3: The monthly averages of tropospheric NO_2 global density for the period from January 2019 to December 2021.

	NO_2 column density (μmol/m^2)		
Month	2019	2020	2021
January	55.3	53.9	53.7
February	52.3	49.7	50.6
March	49.1	46.8	48.2
April	51.0	48.6	50.2
May	55.3	52.3	54.5
June	58.4	55.4	57.1
July	55.9	54.4	57.0
August	51.6	51.2	53.2
September	48.1	47.4	49.1
October	49.3	48.3	49.6
November	53.8	50.9	52.9
December	55.5	55.3	55.9

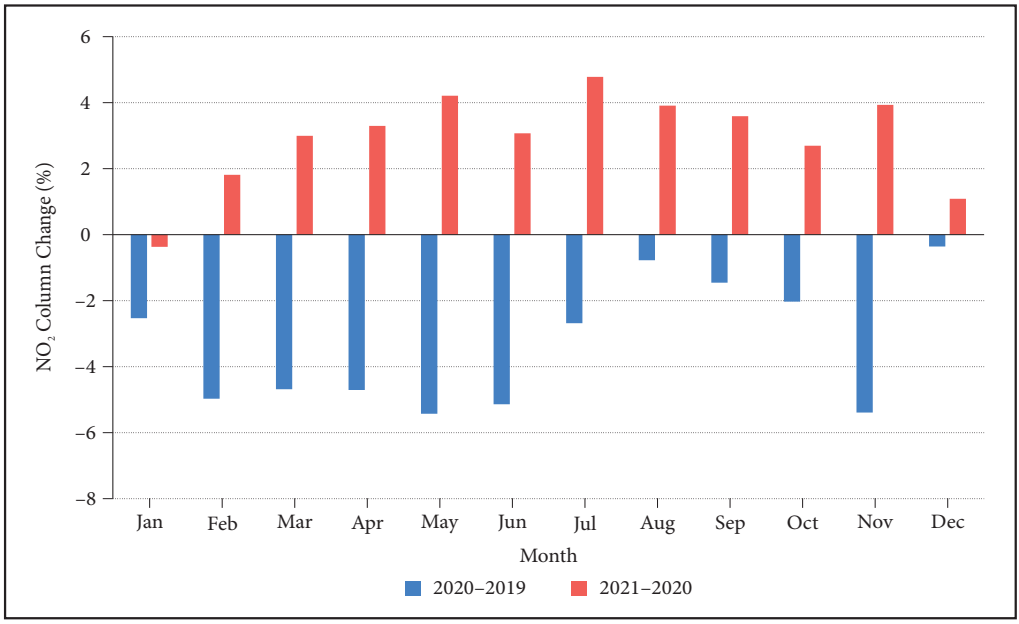

Figure 4: The percentage differences between 2020–2019 and 2021–2020 of global monthly averages of tropospheric NO_2 concentrations for the same month.

3.2 NO_2 emissions on the continents

The annual averages of NO_2 emissions by continent for the years 2019, 2020 and 2021 are presented in Table 2. The ranking in 2019, from the highest to the lowest, is as follows: Europe, Asia, North America, Oceania, Africa and South America. The ranking remains unchanged in 2020, but Oceania regresses one place and Africa rises one in 2021. In comparison to 2019, NO_2 emissions in 2020, the year during which pandemic restrictions were most strictly applied, decreased by 8.7% in Europe, 6.1% in Asia, 4.8% in North America, 1.0% in Africa, while they increased by 0.9% in Oceania and 3.5% in South America. In 2021, NO_2 emissions exhibited an increase of 9.2% in Europe, 7.0% in Asia, 3.1% in North America, 5.3% in Africa, and 1.2% in South America in comparison to 2020. The only decrease was observed in Oceania, where emissions decreased by 2.6%. Between 2021 and 2019, NO_2 emissions decreased by 0.3% in Europe, 1.8% in North America and 1.7% in Oceania, while it increased 0.5% in Asia, 4.2% in Africa, and 4.8% in South America. South America was the only continent whose averages exhibited an increase in both years.

Table 4 presents the monthly averages of NO_2 column densities for the continents from January 2019 to December 2021. With regard to Africa, it can be observed that NO_2 emissions decreased until August 2020 and then increased continuously until the end of the study period (Figure 5a). For Asia, NO_2 emissions exhibited a decrease for all months except December in 2020, followed by an increase for all months except December in 2021 (Figure 5b). In Europe, NO_2 emissions exhibited a decrease until December 2020, followed by a continuous increase (Figure 5c). Among all the continents, the greatest change in NO_2 levels between consecutive years was observed in Europe, with a 40% increase between February 2020 and 2021. For North America, a downward trend is observed across all of 2020, with the exception of November, and an upward trend across 2021, with the exception of January, February and November (Figure 5d). In contrast to the other continents, the tropospheric NO_2 values in Oceania and South America did not decline until May 2020, in comparison to the values observed in 2019. From that point onwards, the values exhibited a variable trend in Oceania and South America (Figure 5e and 5f). Moreover, the magnitudes of change were relatively modest in comparison to those observed in other continents.

The results demonstrate that human-induced NO_2 emissions have undergone corresponding changes across continents during the pandemic process, particularly in relation to the extent of their industrialisation based on fossil fuels. In the study of Cooper et al. (2022), the emission estimates for 2020, which were made by considering the ten-year period prior to the pandemic, were compared with the new situation resulting from the actual pandemic for the continents. Accordingly, the largest discrepancy from the projected values was identified for Europe, corroborating the findings of our investigation.

3.3 NO_2 emissions in countries as grouped according to HDI

The annual changes of NO_2 emissions for countries in categories classified according to the HDI are presented in Table 2. Accordingly, in 2019, the category ranking from high to low is *Very High*, *High*, *Medium* and *Low*. The ranking remains unchanged in 2020, but in 2021 the total emissions of the *High* category exceed those of the *Very High* category. In 2020, when pandemic restrictions were the most stringent, there was a reduction in NO_2 emissions across all categories in comparison to 2019. The decline in the *Very High* category was 5.1%, in the *High* category 3.7%, in the *Medium* category 2.0%, and in the *Low* category 1.5%. In 2021, NO_2 emissions exhibited an increase in all categories when compared to 2020. The increase was 4.7% in the *Very High* category, 5.7% in the *High* category, 6.2% in the *Medium* category, and 7.2% in the *Low* category. A comparison of the 2021 averages with those of 2019 reveals that total NO_2 emissions decreased only in the *Very High* category (0.6%) and increased in all other categories (*High*: 1.9%, *Medium*: 4.1%, *Low*: 5.6%) in 2021. The results of the 2020–2019 period indicate that the reduction in NO_2 emissions is more pronounced in regions with a higher development index. Conversely, the results for the period 2021–2020 indicate a greater rate of increase in emissions in regions with a lower HDI. This suggests that the severity of the closures may be increasing in line with the development level.

Figure 5: The monthly percentage differences of NO_2 column concentrations of a) Africa, b) Asia, c) Europe, d) North America, e) Oceania, f) South America between consecutive years, 2020–2019 and 2021–2020. ► p. 86

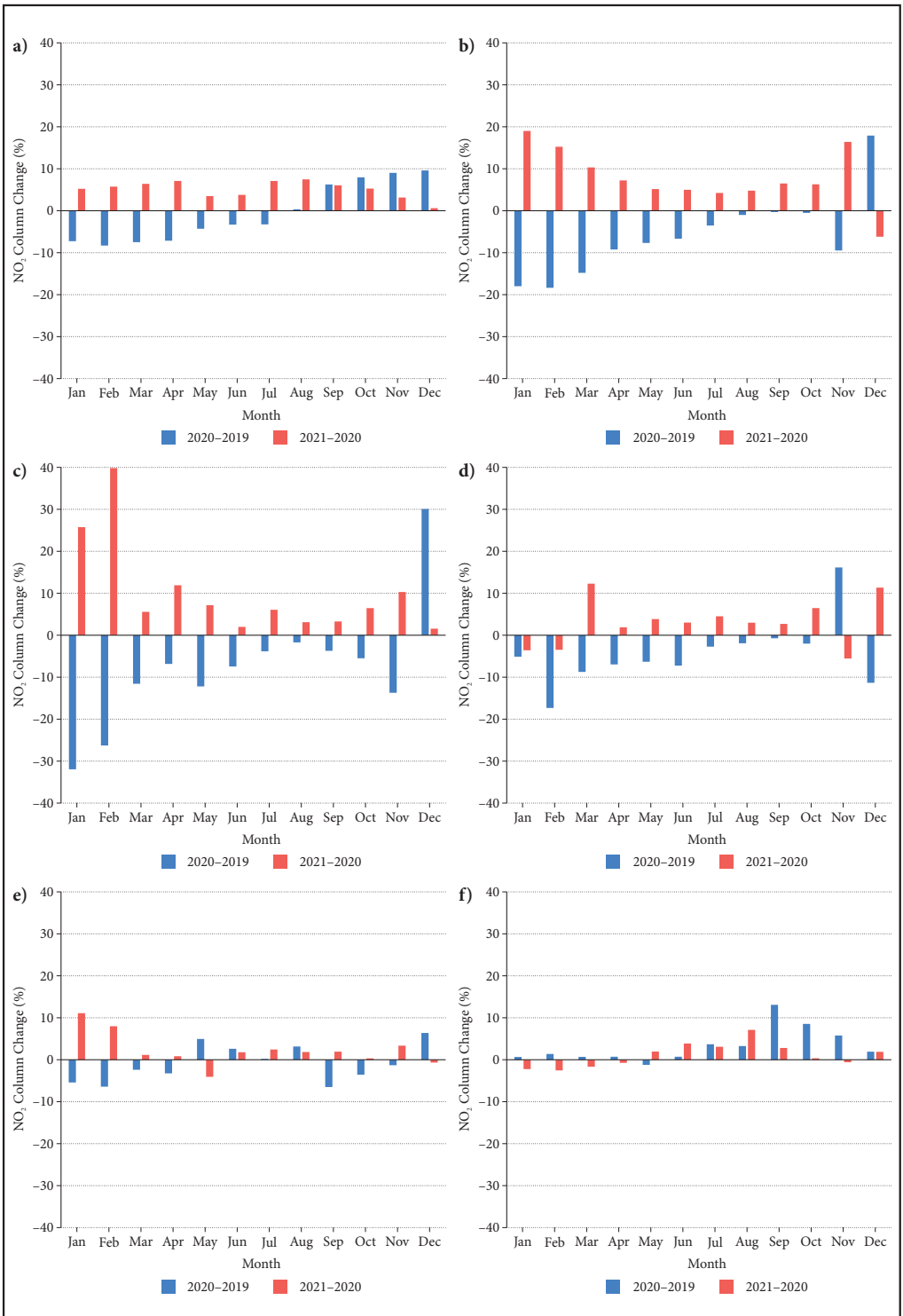
a)
b)
c)
d)
e)
f)
NO2 Column Change (%)
40
30
20
10
0
−10
−20
−30
−40
Jan Feb Mar Apr May Jun Jul Aug Sep Oct Nov Dec
Month
2020–2019
2021–2020

Table 4: The monthly averages of NO_2 column densities of the continents for the period from January 2019 to December 2021.

	NO_2 column density (µmol/m^2)																	
	Africa			Asia			Europe			N. America			S. America			Oceania		
Month	2019	2020	2021	2019	2020	2021	2019	2020	2021	2019	2020	2021	2019	2020	2021	2019	2020	2021
Jan.	49.5	45.9	48.3	65.5	53.7	63.9	83.9	57.1	71.8	41.3	39.2	37.8	45.1	45.4	44.4	57.2	60.3	53.6
Feb.	49.4	45.3	47.9	57.1	46.6	53.7	74.6	55.0	76.9	49.1	40.6	39.2	43.1	43.7	42.6	53.0	56.4	51.9
Mar.	50.7	46.9	49.9	62.7	53.4	58.9	70.9	62.7	66.2	48.1	43.9	49.3	42.6	42.9	42.2	50.3	51.5	50.9
Apr.	51.7	48.0	51.4	70.3	63.8	68.4	73.1	68.1	76.2	62.0	57.7	58.8	41.4	41.7	41.4	46.4	47.9	47.5
May	53.7	51.4	53.2	75.5	69.7	73.3	84.4	74.1	79.4	74.6	69.9	72.6	41.1	40.6	41.4	46.4	44.1	45.9
June	57.5	55.6	57.7	79.5	74.2	77.9	87.4	80.9	82.5	81.7	75.8	78.1	40.9	41.2	42.8	45.7	44.5	43.7
July	58.4	56.5	60.5	76.0	73.3	76.4	80.7	77.6	82.3	77.2	75.1	78.5	43.4	45.0	46.4	45.3	45.2	44.1
Aug.	56.0	56.2	60.4	67.7	67.0	70.2	75.4	74.1	76.4	68.0	66.7	68.7	49.0	50.6	54.2	50.5	48.9	48.0
Sep.	52.8	56.1	59.5	58.9	58.7	62.5	70.0	67.4	69.6	55.6	55.2	56.7	50.4	57.0	58.6	53.8	57.3	56.2
Oct.	49.1	53.0	55.8	55.9	55.6	59.1	65.5	61.9	65.9	45.6	44.7	47.6	50.2	54.5	54.7	58.9	61.0	60.8
Nov.	46.6	50.8	52.4	57.9	52.4	61.0	61.9	53.4	58.9	39.0	45.3	42.8	48.5	51.3	51.0	61.8	62.6	60.5
Dec.	45.9	50.3	50.6	58.6	69.1	64.8	59.5	77.4	78.6	39.7	35.2	39.2	46.8	47.7	48.6	62.6	58.6	59.0

Table 5: The monthly averages of NO_2 column densities of the HDI categories for the period from January 2019 to December 2021.

	NO_2 column density (μmol/m^2)											
	Very High HDI			High HDI			Medium HDI			Low HDI		
Month	2019	2020	2021	2019	2020	2021	2019	2020	2021	2019	2020	2021
Jan.	56.9	50.7	53.3	63.0	51.7	59.8	53.7	49.5	52.7	48.8	43.7	48.7
Feb.	55.5	47.6	52.8	59.8	49.3	53.7	53.8	49.9	53.8	48.7	43.6	47.1
Mar.	56.6	51.3	54.7	61.1	54.6	58.2	57.7	52.5	58.5	49.9	45.7	50.0
Apr.	63.6	59.4	62.7	61.0	57.6	60.9	58.8	53.9	58.9	51.3	47.2	50.8
May	70.8	65.1	68.6	62.5	58.9	61.3	61.4	57.4	59.8	52.3	49.5	52.7
June	74.8	70.0	72.2	63.3	60.1	63.1	65.0	61.7	64.6	55.2	52.3	55.7
July	71.8	69.6	72.2	62.0	60.9	64.1	64.8	62.0	66.9	54.6	52.2	56.8
Aug.	66.2	65.5	67.3	61.5	60.4	65.0	61.6	61.4	65.9	51.5	51.4	55.9
Sep.	59.1	59.3	61.3	58.9	61.3	65.1	58.2	61.4	64.9	48.7	51.4	55.3
Oct.	55.3	54.0	57.2	57.6	60.4	62.7	53.8	57.3	60.6	45.8	50.1	53.1
Nov.	53.1	50.2	53.7	56.3	57.3	61.0	50.8	54.0	56.3	44.7	49.4	52.0
Dec.	52.8	56.6	56.3	55.0	63.1	60.6	49.4	54.3	54.1	43.9	49.7	50.5

Table 5 presents the monthly averages of NO_2 column densities for countries belonging to different HDI categories for the period from January 2019 to December 2021. The NO_2 emissions in the *Very High* category exhibited a downward trend for the majority of months in 2020, with the exception of September and December. Conversely, an upward trend was observed for all months in 2021, with the exception of December (Figure 6a). In this category, the greatest reductions and increases in NO_2 emissions for the study period were observed in February 2020 and February 2021, respectively. In the *High* category, NO_2 emissions exhibited a pronounced decline in the initial months of 2020, followed by an upward trend from September of the same year. This upward trend persisted until December 2021, as illustrated in Figure 6b. Among all categories, the greatest reduction and increase in emissions for the entire study period were observed in the *High* category in January 2020 and January 2021, respectively. In the *Medium* and *Low* HDI categories, a reduction in emissions was observed in 2020 until September. Subsequently, emissions exhibited an upward trend until the end of 2021 (Figures 6c and 6d).

Following the implementation of measures to combat the epidemic, there was an uninterrupted decline in emissions over an extended period. However, this trend was reversed in September 2020, with emissions increasing in all categories except the *Very High* category. The reversal of this trend commenced in December 2020 for the *Very High* category, suggesting that the relaxation of lockdowns in countries in this category lagged behind by a few months.

A substantial majority of studies analysing the impacts of the pandemic on pollutant emissions have examined the situation at the scale of cities and countries. In contrast, Li et al. (2022), employing a data-driven approach, analysed regions without limiting them to administrative boundaries. Their findings indicated that these regions can be divided into three distinct clusters according to their pollution levels. The findings of the study indicated that the level of restriction measures in the cluster with the highest emissions was more stringent than in the other clusters, and NO_2 emissions in this cluster declined more than in the others. A comparison of the results of our study with those of this study revealed that a significant number of countries in the *Very High* and *High* HDI categories corresponded to the cluster designated as poor (with the highest emissions) in this study.

3.4 NO_2 emissions in Slovenia, Croatia, and Bosnia and Herzegovina

In the last phase of the study, tropospheric NO_2 levels were monitored in three neighbouring southern European countries: Slovenia, Croatia, Bosnia and Herzegovina (Figure 7a). Slovenia (population approximately 2.1 million) and Croatia (population approximately 3.8 million) are classified as belonging to the

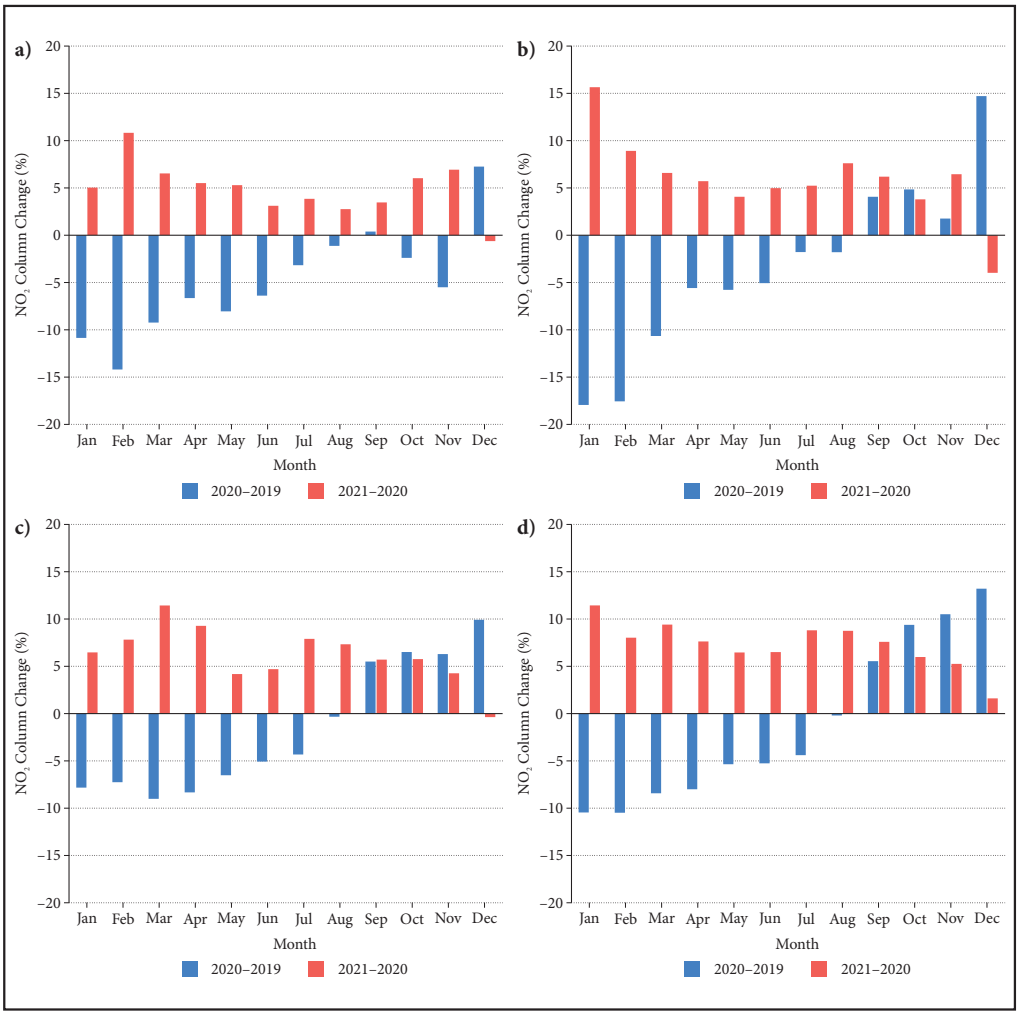

Figure 6: The monthly percentage differences of NO_2 column concentrations of a) *Very High* b) *High* c) *Medium* d) *Low* developed countries between consecutive years, 2020–2019 and 2021–2020.

Very High HDI category, while Bosnia and Herzegovina (population approximately 3.2 million) classified as belonging to the *High* HDI category. The distributions of annual average tropospheric NO_2 levels in these three countries for the pre-pandemic year (2019), pandemic year (2020) and post-pandemic year (2021) are presented in Figures 7b, 7c and 7d, respectively. The annual average of NO_2 over Bosnia and Herzegovina is consistently lower than the other two countries, in line with the values presented in Table 2. The impact of pandemic measures on NO_2 emissions is evident when comparing Figures 7b and 7c for all three countries. Table 2 also indicates that there was a decrease of 5.9% for Slovenia, 6.1% for Croatia and 6.3% for Bosnia and Herzegovina in 2020 compared to 2019. In 2021, the increases in NO_2 emissions following the removal of measures are revealed by comparing Figures 7c and 7d. The annual averages increased by 10.5% for Slovenia, 9.6% for Croatia and 10.3% for Bosnia and Herzegovina in 2021 compared

Figure 7: a) Slovenia-Croatia-Bosnia and Herzegovina triad on the map and their annual average of tropospheric NO_2 column densities for the year b) 2019, c) 2020, d) 2021. ► p. 90

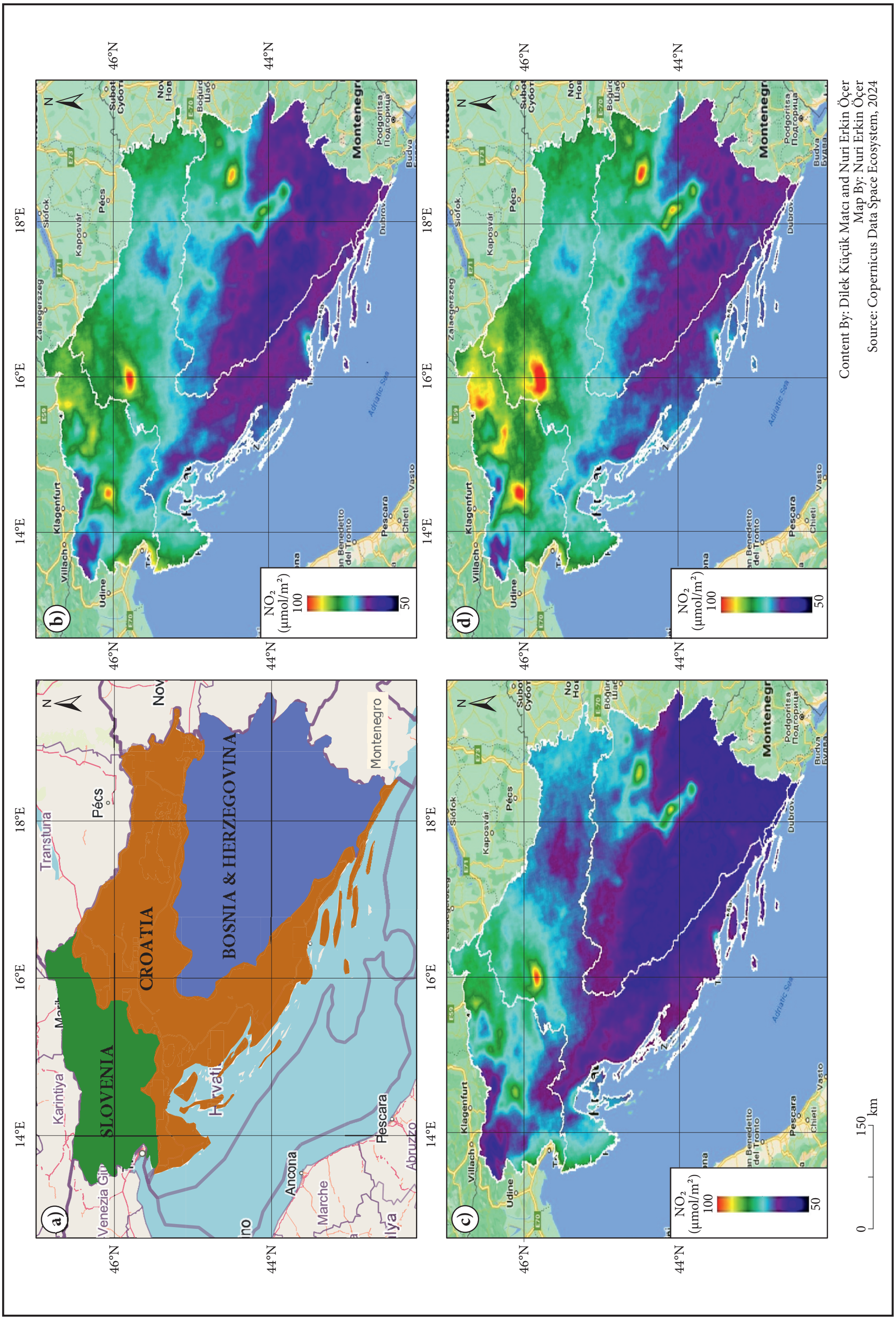
a)
SLOVENIA
CROATIA
BOSNIA & HERZEGOVINA
b)
c)
d)
NO_2 (µmol/m²)
100
50
46°N
44°N
14°E
16°E
18°E
0
150 km
Content By: Dilek Küçük Matcı and Nuri Erkin Öçer
Map By: Nuri Erkin Öçer
Source: Copernicus Data Space Ecosystem, 2024

to 2020, as indicated by Table 2. A comparison of the 2021 averages with those of 2019 reveals that there were net increases of 4.0% in Slovenia, 3.0% in Croatia and 3.4% in Bosnia and Herzegovina.

The monthly averages of the NO_2 column densities for these countries for the months from January 2019 to December 2021 are presented in Table 6 and the monthly percentage differences of the NO_2 column concentrations of each country between the consecutive years 2020–2019 and 2021–2020 are presented in Figure 8. According to information reflected in reports by organisations such as the Inter-university Consortium for Political and Social Research (ICPSR) and the Organisation for Economic Cooperation and Development (OECD), in response to the initial cases of coronavirus that emerged in early March 2020 and the subsequent rapid spread of the virus, the governments of all three countries implemented a series of measures with the aim of halting the spread from mid-March onwards. These measures included the closure of educational institutions, limitations on public gatherings, the closure of cafes, restaurants and non-essential shops, and the imposition of travel restrictions. The implementation of these measures, which significantly restrict human mobility (Brezina et al. 2021), has resulted in a downward trend in human-induced NO_2 emissions in the atmosphere during the pandemic year, as illustrated in Figure 8. Following the control of the outbreak, the measures were eased in Bosnia and Herzegovina at the end of April and in Slovenia and Croatia from mid-May. Consequently, the reduction in emissions has slowed down. Nevertheless, following the relaxation of restrictions, the number of infected individuals in Slovenia and Croatia increased exponentially from October, leading to a further tightening of measures in November. Consequently, NO_2 emissions for these two countries fell rapidly again in November. A comparison of 2020 and 2019 November emission values confirms this result. In Bosnia and Herzegovina, the number of infected cases continued to increase linearly, and there was no further tightening of measures. Consequently, the decline in NO_2 emissions in Bosnia and Herzegovina has been considerably less pronounced than in the other two countries. Following the relaxation of restrictions in 2021, there was a notable increase in human mobility across all three countries, which led to a corresponding rise in NO_2 emissions.

Table 6: The monthly averages of NO_2 column densities of Slovenia, Croatia, Bosnia and Herzegovina for the period from January 2019 to December 2021.

	NO_2 column density (μmol/m^2)								
	2019			2020			2021		
	Slovenia	Croatia	Bosnia and Herzegovina	Slovenia	Croatia	Bosnia and Herzegovina	Slovenia	Croatia	Bosnia and Herzegovina
Jan	76.5	67.4	61.0	82.0	62.1	52.0	88.5	74.4	66.4
Feb	89.9	71.8	67.7	74.6	65.4	57.9	77.9	62.0	54.1
Mar	81.9	74.0	66.6	72.2	67.9	63.6	85.4	75.1	70.2
Apr	89.9	85.2	77.1	69.6	69.3	68.0	85.8	81.9	74.9
May	91.1	85.2	76.6	77.3	73.3	68.7	78.5	74.7	71.7
Jun	83.3	83.4	80.6	75.9	74.4	71.0	80.7	80.1	76.6
Jul	81.3	81.3	77.6	77.4	75.7	73.0	78.1	77.8	76.0
Aug	78.3	78.3	75.4	78.0	76.9	72.7	77.3	76.6	73.7
Sep	79.0	74.6	70.5	75.5	73.4	68.8	79.5	76.8	72.2
Oct	72.8	67.2	63.7	71.3	68.4	63.1	85.5	81.0	78.3
Nov	75.1	63.1	55.3	60.9	55.7	53.4	91.8	81.3	72.3
Dec	69.6	60.8	54.8	96.7	75.7	62.9	98.1	77.1	68.3

Figure 8: The monthly percentage differences of NO_2 column concentrations of a) Slovenia b) Croatia c) Bosnia and Herzegovina between consecutive years, 2020–2019 and 2021–2020. ► p. 92

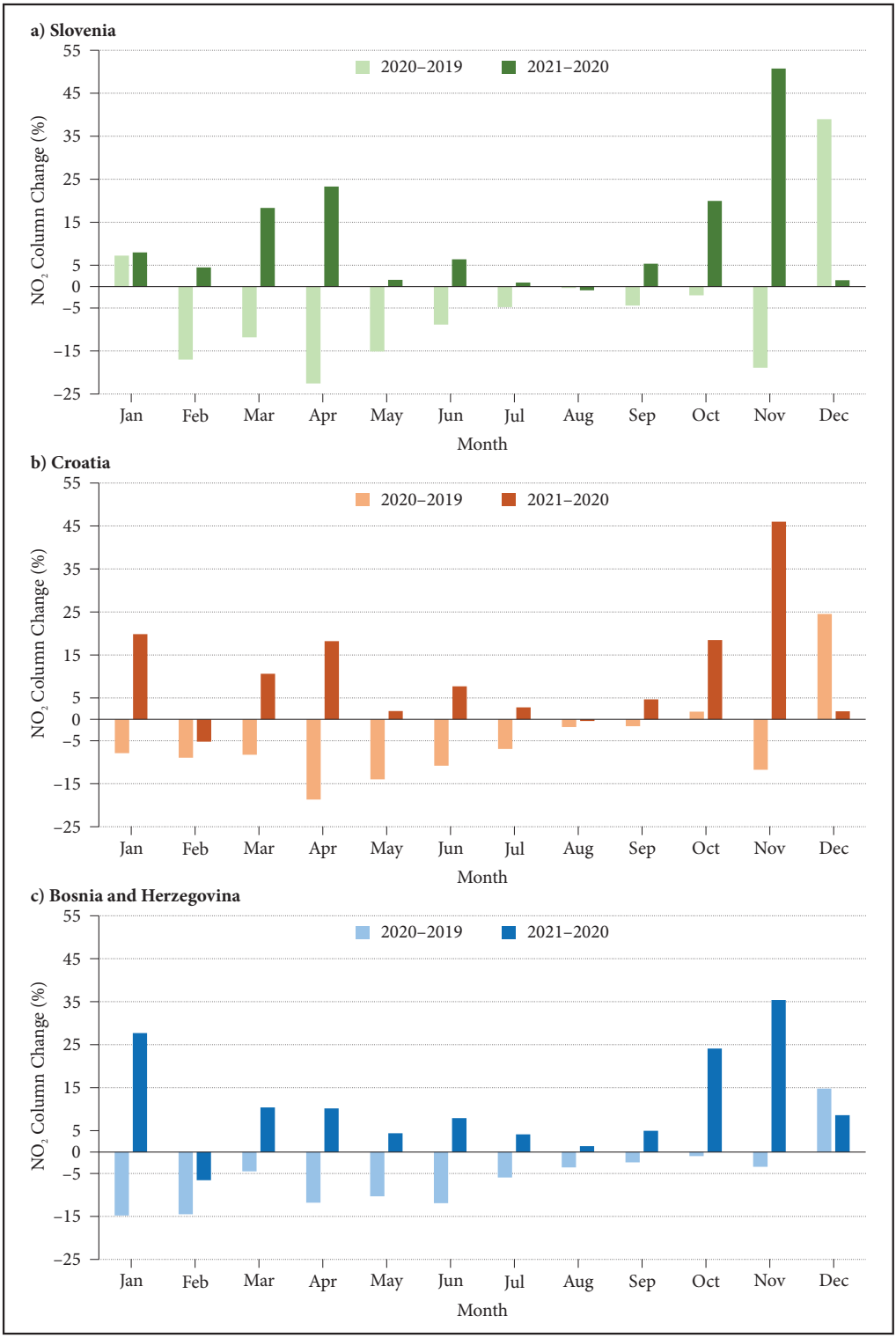
a) Slovenia
2020–2019
2021–2020
NO2 Column Change (%)
55
45
35
25
15
5
0
–5
–15
–25
Jan
Feb
Mar
Apr
May
Jun
Jul
Aug
Sep
Oct
Nov
Dec
Month
b) Croatia
2020–2019
2021–2020
NO2 Column Change (%)
Month
c) Bosnia and Herzegovina
2020–2019
2021–2020
NO2 Column Change (%)
Month

4 Conclusions

In this study, TROPOMI data were accessed and processed through Google Earth Engine (GEE) in order to monitor and evaluate the effects of the COVID-19 pandemic on tropospheric NO_2 concentrations and distributions at various supranational scales. The study examines the levels of NO_2 in countries grouped according to the Human Development Index (HDI), as well as the temporal variation of NO_2 across the globe, continents and the triad of Slovenia, Croatia, and Bosnia and Herzegovina.

The results of the study indicate a notable decline in NO_2 levels across all study areas during the pandemic period in comparison to the pre-pandemic period. The decline commenced even before the implementation of restrictions and closures by governments. In contrast to other studies, the results of our study indicate that the observed reductions in emissions in the period before the implementation of the restrictions, i.e. in the first three months of 2020, cannot be attributed solely to the adoption of the measures. Instead, it appears that individuals are also adopting behaviours to protect themselves from the disease, such as avoiding social contact and limiting their own mobility in the community, and that emissions are starting to fall as a result.

Following a prolonged period of decline, emissions began to increase across all HDI categories and on most continents (with the exception of Oceania and South America) in response to the relaxation and removal of the measures and associated increased human mobility. The increase trend commenced three months earlier in the *High*, *Medium* and *Low* HDI categories than in the *Very High* category, indicating an earlier relaxation of lockdowns in these countries. Another noteworthy finding of the study is that during the period of restrictions, the decline in NO_2 emissions increases as the development index increases. Furthermore, the results for the period following the lifting of restrictions indicate that the rate of increase in emissions is greater in areas with a lower HDI. These two observations were interpreted as the severity of closures increases as the level of development increases.

In the final phase of the study, tropospheric NO_2 levels were monitored in Slovenia, Croatia, and Bosnia and Herzegovina before, during and after the pandemic. Although the pre-pandemic level of emissions in Bosnia and Herzegovina, which is in the *High* HDI category, was significantly lower than in the other two *Very High* HDI countries, it demonstrated similar trends to the pandemic emissions in the other two countries. However, variations in outcomes were also observed in relation to the timing of the implementation of measures.

The results demonstrate that a study requiring the access of thousands of data and the use of terabytes of memory can be successfully conducted through a cloud-based software such as GEE. The processes that would have required considerable resources, time, and labour, and would have been error-prone without GEE, were executed efficiently through this platform in the course of the research.

5 References

Ataey, A., Jafarvand, E., Adham, D., Moradi-Asl, E. 2020: The relationship between obesity, overweight, and the human development index in world health organization eastern mediterranean region countries. *Journal of Preventive Medicine and Public Health* 53-2. https://doi.org/10.3961/jpmph.19.100

Avdan, U., Kaplan, G., Avdan, Z., Matcı, D., Erdem, F., Mızık, E., Ozudogru, I. 2021: Comparison of remote sensing soil electrical conductivity from planetscope and ground measured data in wheat and beet yields. *Biology and Life Sciences Forum* 3-1. https://doi.org/10.3390/IECAG2021-09741

Bacak, T., Dursun, Ş., Toros, H. 2020: The effect of COVID-19 outbreak on air quality of Istanbul city centre. *Journal of Research in Atmospheric Science 2*-1.

Brezina, T., Tiran, J., Ogrin, M., Laa, B. 2021: COVID-19 impact on daily mobility in Slovenia. *Acta geographica Slovenica* 61-2. https://doi.org/10.3986/AGS.9390

Cooper, M., Martin, R., Hammer, M., Levelt, P., Veefkind, P., Lamsal, L., Krotkov, N. A. et al. 2022: Global fine-scale changes in ambient NO_2 during COVID-19 lockdowns. *Nature 601*. https://doi.org/10.1038/s41586-021-04229-0

Hale, T., Angrist, N., Goldszmidt, R., Kira, B., Petherick, A., Phillips, T., Webster, S. et al. 2021: A global panel database of pandemic policies (Oxford COVID-19 Government Response Tracker). *Nature Human Behaviour* 5-4. https://doi.org/10.1038/s41562-021-01079-8

Isaifan, R. 2020: The dramatic impact of Coronavirus outbreak on air quality: Has it saved as much as it has killed so far? *Global Journal of Environmental Science and Management* 6-3. https://doi.org/10.22034/gjesm.2020.03.01

Jalayer, S., Sharifi, A., Abbasi-Moghadam, D., Tariq, A., Qin, S. 2023: Assessment of spatiotemporal characteristic of droughts using *in situ* and remote sensing-based drought indices. *IEEE Journal of Selected Topics in Applied Earth Observations and Remote Sensing* 16. https://doi.org/10.1109/JSTARS.2023.3237380

Karuppasamy, M., Seshachalam, S., Natesan, U., Ayyamperumal, R., Karuppannan, S., Gopalakrishnan, G., Nazir, N. 2020: Air pollution improvement and mortality rate during COVID-19 pandemic in India: global intersectional study. *Air Quality, Atmosphere & Health* 13-11. https://doi.org/10.1007/s11869-020-00892-w

Kumar, L., Mutanga, O. 2019: Google Earth Engine applications. MDPI. https://doi.org/10.3390/books978-3-03897-885-5

Kuruca, M., Matci, D., Uğur, A. 2021: The potential of Göktürk 2 satellite images for mapping burnt forest areas. *Turkish Journal of Agriculture and Forestry* 45-1. https://doi.org/10.3906/tar-2001-79

Li, Y., Li, M., Rice, M., Yang, C. 2022: Impact of COVID-19 containment and closure policies on tropospheric nitrogen dioxide: A global perspective. *Environment International* 158. https://doi.org/10.1016/j.envint.2021.106887

Lian, X., Huang, J., Huang, R., Liu, C., Wang, L., Zhang, T. 2020: Impact of city lockdown on the air quality of COVID-19-hit of Wuhan city. *Science of the Total Environment* 742. https://doi.org/10.1016/j.scitotenv.2020.140556

Long, X., Yu, H., Sun, M., Wang, X., Klemeš, J., Xie, W., Wang, C. et al. 2020: Sustainability evaluation based on the Three-dimensional Ecological Footprint and Human Development Index: A case study on the four island regions in China. *Journal of Environmental Management* 265. https://doi.org/10.1016/j.jenvman.2020.110509

Matci, D., Avdan, U. 2020: Comparative analysis of unsupervised classification methods for mapping burned forest areas. *Arabian Journal of Geosciences* 13-15. https://doi.org/10.1007/s12517-020-05670-7

Matci, D., Comert, R., Avdan, U. 2020: Comparison of tree-based classificatıon algorıthms in mapping burned forest areas. *Geodetski vestnik* 64-3. https://doi.org/10.15292/geodetski-vestnik.2020.03.348-360

Nejad, S., Abbasi-Moghadam, D., Sharifi, A., Farmonov, N., Amankulova, K., László, M. 2022: Multispectral crop yield prediction using 3D-convolutional neural networks and attention convolutional LSTM approaches. *IEEE Journal of Selected Topics in Applied Earth Observations and Remote Sensing* 16. https://doi.org/10.1109/JSTARS.2022.3223423

Nemati, M., Ebrahimi, B., Nemati, F. 2020: Assessment of Iranian nurses' knowledge and anxiety toward COVID-19 during the current outbreak in Iran. *Archives of Clinical Infectious Diseases* 15. https://doi.org/10.5812/archcid.102848

Nghia, B., Pal, I., Chollacoop, N., Mukhopadhyay, A. 2022: Applying Google Earth Engine for flood mapping and monitoring in the downstream provinces of Mekong river. *Progress in Disaster Science* 14. https://doi.org/10.1016/j.pdisas.2022.100235

Otmani, A., Benchrif, A., Tahri, M., Bounakhla, M., El Bouch, M., Krombi, M. 2020: Impact of COVID-19 lockdown on PM_{10}, SO_2 and NO_2 concentrations in Salé city (Morocco). *Science of the Total Environment* 735. https://doi.org/10.1016/j.scitotenv.2020.139541

Praticò, S., Solano, F., Di Fazio, S., Modica, G. 2021: Machine learning classification of Mediterranean forest habitats in Google Earth Engine based on seasonal Sentinel-2 time-series and input image composition optimisation. *Remote Sensing* 13-4. https://doi.org/10.3390/rs13040586

Saha, L., Kumar, A., Kumar, S., Korstad, J., Srivastava, S., Bauddh, K. 2022: The impact of the COVID-19 lockdown on global air quality: A review. *Environmental Sustainability* 5-1. https://doi.org/10.1007/s42398-021-00213-6

Sannigrahi, S., Kumar, P., Molter, A., Zhang, Q., Basu, B., Basu, A., Pilla, F. 2021: Examining the status of improved air quality in world cities due to COVID-19 led temporary reduction in anthropogenic emissions. *Environmental research* 196. https://doi.org/10.1016/j.envres.2021.110927

Sarkodie, S., Adams, S. 2020: Electricity access, human development index, governance and income inequality in Sub-Saharan africa. *Energy Reports* 6. https://doi.org/10.1016/j.egyr.2020.02.009

Sharifi, A., Felegari, S. 2022: Nitrogen dioxide (NO_2) pollution monitoring with Sentinel-5P satellite imagery over during the coronavirus pandemic (case study: Tehran). *Remote Sensing Letters* 13-10. https://doi.org/10.1080/2150704X.2022.2120780

Singh, R., Chauhan, A. 2020: Impact of lockdown on air quality in India during COVID-19 pandemic. *Air Quality, Atmosphere & Health* 13-8. https://doi.org/10.1007/s11869-020-00863-1

Tobías, A., Carnerero, C., Reche, C., Massagué, J., Via, M., Minguillón, M., Alastuey, A. et al. 2020: Changes in air quality during the lockdown in Barcelona (Spain) one month into the SARS-CoV-2 epidemic. *Science of the total environment* 726. https://doi.org/10.1016/j.scitotenv.2020.138540

Tok, E., Kaya, S. 2014: Monitoring components of urban environment using vegetation-impervious-soil model and remotely sensed data. *Journal of Environmental Protection and Ecology* 15-4.

Verhoelst, T., Compernolle, S., Pinardi, G., Lambert, J., Eskes, H., Eichmann, K., Fjæraa, A. et al. 2020: Ground-based validation of the copernicus Sentinel-5P TROPOMI NO_2 measurements with the NDACC ZSL-DOAS, MAX-DOAS and Pandonia global networks. *Atmospheric Measurement Techniques Discussions* 14-1. https://doi.org/10.5194/amt-14-481-2021

Waleed, M., Sajjad, M., Shazil, M., Tariq, M., Alam, M. 2023: Machine learning-based spatial-temporal assessment and change transition analysis of wetlands: An application of Google Earth Engine in Sylhet, Bangladesh (1985–2022). *Ecological Informatics* 75. https://doi.org/10.1016/j.ecoinf.2023.102075

Xiong, J., Thenkabail, P., Gumma, M., Teluguntla, P., Poehnelt, J., Congalton, R., Yadav, K. et al. 2017: Automated cropland mapping of continental Africa using Google Earth Engine cloud computing. *ISPRS Journal of Photogrammetry and Remote Sensing* 126. https://doi.org/10.1016/j.isprsjprs.2017.01.019

Zhang, H., Lin, Y., Wei, S., Loo, B., Lai, P., Lam, Y., Wan, L. et al. 2021: Global association between satellite-derived nitrogen dioxide (NO_2) and lockdown policies under the COVID-19 pandemic. *Science of The Total Environment* 761. https://doi.org/10.1016/j.scitotenv.2020.144148

Zhe, W. 2018: Remote sensing estimation of daily average temperature in northwestern China based on advanced microwave scanning radiometer for the Earth observing system. *Journal of Environmental Protection and Ecology* 19-3